ADVANCES IN ATMOSPHERIC SCIENCES, VOL. 29, NO. 4, 2012, 661–674

A Possible Mechanism of the Impact of Atmosphere–Ocean Interaction on the Activity of Tropical Cyclones Affecting China

REN Fumin*[1] (任福民), BAI Lina[2,3] (白莉娜), WU Guoxiong[4] (吴国雄), WANG Zaizhi[1] (王在志), and WANG Yuan[2] (王 元)

[1]*Laboratory for Climate Studies, China Meteorological Administration, Beijing* 100081

[2]*Key Laboratory of Mesoscale Severe Weather of Ministry of Education, Nanjing University, Nanjing* 210093

[3]*Shanghai Typhoon Institute, China Meteorological Adminstration, Shanghai* 200030

[4]*Atmospheric Physics Research Institute of Chinese Academy of Sciences, Beijing* 100029

(Received 19 July 2011; revised 5 January 2012)

ABSTRACT

In this study, tropical cyclone data from China Meteorological Administration (CMA) and the ECMWF reanalysis data for the period 1958–2001 was used to propose a possible mechanism for the impacts of air–sea interaction on the activity of tropical cyclones (TCs) affecting China. The frequency of TCs affecting China over past 40 years has trended downward, while during the same period, the air–sea interaction in the two key areas of the Pacific region has significantly weakened. Our diagnoses and simulations suggest that air–sea interactions in the central North Pacific tropics and subtropics (Area 1) have an important role in adjusting typhoon activities in the Northwest Pacific in general, and especially in TC activity affecting China. On the contrary, impacts of the air–sea interaction in the eastern part of the South Pacific tropics (Area 2) were found to be rather limited. As both observational analysis and modeling studies show that, in the past four decades and beyond, the weakening trend of the latent heat released from Area 1 matched well with the decreasing Northwest Pacific TC frequency derived from CMA datasets. Results also showed that the weakening trend of latent heat flux in the area was most likely due to the decreasing TC frequency over the Northwest Pacific, including those affecting China. Although our preliminary analysis revealed a possible mechanism through which the air–sea interaction may adjust the genesis conditions for TCs, which eventually affect China, other relevant questions, such as how TC tracks and impacts are affected by these trends, remain unanswered. Further in-depth investigations are required.

Key words: air–sea interaction, latent heat, affecting China tropical cyclones, impact mechanism

Citation: Ren, F. M., L. N. Bai, G. X. Wu, Z. Z. Wang, and Y. Wang, 2012: A possible mechanism of the impact of air–sea interaction on the activity of tropical cyclones affecting China. *Adv. Atmos. Sci.*, **29**(4), 661–674, doi: 10.1007/s00376-012-1028-9.

1. Introduction

The water vapor and energy of tropical cyclones (TCs) come mainly from the ocean, and the ocean and air–sea interaction then affect TC climate change. Palmén (1948) pointed out that the regions where sea surface temperature (SST) is higher than 26.5°C are favorable for TC genesis. Chan and Liu (2004) found a strong positive relationship between the typhoon activity in the western North Pacific (WNP) and SSTs over the equatorial eastern Pacific Ocean. Such interannual variations of typhoon activity appear to be largely constrained by large-scale atmospheric factors including low-level vorticity, vertical wind shear, and

*Corresponding author: REN Fumin, fmren@163.com

moist static energy. Chan (2006, 2008) concluded that the local SSTs in the western North Pacific are not a significant factor in determining the TC activity in the region. Hoyos et al. (2006) indicated that the increasing trend of category 4 and 5 hurricanes is mainly related to SSTs. Results of many numerical models (Haarsma et al., 1993; Krishnamurti et al., 1998) have also indicated that TC frequency increases with higher SSTs. Many previous studies have mainly focused on the influence of SST on TC activity climate change in the Northwest Pacific. However, SSTs cannot fully represent the force function of the ocean to the atmosphere.

In the air–sea coupled system, the ocean influences atmospheric motion mainly through heat transportation, especially latent heat flux (Li, 2000; Zhou and Zhang, 2002). The sensible heat and latent heat flux from the ocean to the atmosphere are important factors for TC genesis and intensification (Chen and Ding, 1979). Zhang et al. (1994) pointed out that latent heat flux is the main energy source for a mature typhoon but the sensible heat flux almost has no impact on a mature typhoon. Li and Chen (2005) found that both of the latent and sensible heat fluxes are favorable for TC maintenance and enhancement, with the effect of latent heat flux being more remarkable. Ooyama (1969) also emphasized the importance of the latent heat flux for the development of TCs, and suggested that not only the latent heat flux within the TC region but also outside the region need to be considered. Most of the above-mention research was conducted based on a single TC case.

In contrast to previous studies, this study investigated the impact of latent heat flux on the entirety of TC activity in the Northwest Pacific, especially on TCs affecting China[a] from the climatology point of view. By diagnosing the relationship between TC activity and global latent heat flux, the key areas of air–sea interaction for the TC activity in the Northwest Pacific were identified. In addition, we investigated the possible mechanisms behind air–sea interaction in the key areas that influence the atmospheric circulation as well as and TC activity in the Northwest Pacific.

2. Data and analysis methods

Based on an analysis of three TC datasets from the Shanghai Typhoon Institute of China Meteorological Administration (STI-CMA), the U.S. Joint Typhoon Warning Center (JTWC) and Japan Meteorological Agency (JMA), Ren et al. (2012) found that the CMA dataset was relatively more complete and more accurate for TCs affecting China. In this study, the CMA dataset was used, and the environment variables were obtained from the ECMWF reanalysis data.

First, because the maximum heating effect of the ocean to the atmosphere often does not happen directly over the region with the maximum evaporation Li (2000), it was important to find the key region of air–sea interaction. This was determined using two steps: (1) a quantitative analysis of the distribution of global latent heat flux and find the region with maximum latent heat flux, and (2) a relationship analysis between the frequency of TCs affecting China in the Northwest Pacific and the latent heat flux to determine the key regions with high correlation coefficient. Then we analyzed the water vapor budget over the Northwest Pacific and diagnosed the possible mechanism of the impact of latent heat flux on TC activity. Calculations and analyses included in this study are as follows (Ding, 1989; Ding and Hu, 2003).

2.1 *The potential function and stream function of water vapor flux*

Water vapor flux represents the water vapor quantity (grams) flowing through a unit of area in a unit of time, which shows the quantity and direction of the water vapor transport. The water vapor transport is divided into horizontal transport and vertical transport, and the calculation formula of horizontal transport $\boldsymbol{Q}$ is $\boldsymbol{Q} = \frac{1}{g}\boldsymbol{V}q$. Its non-divergence and non-rotational components were obtained by solving the stream function and potential function of horizontal water vapor transport component $\boldsymbol{Q}$:

$$\boldsymbol{Q} = k \times \nabla\Psi + (-\nabla\chi) = \boldsymbol{Q}_\Psi + \boldsymbol{Q}_\chi \,, \tag{1}$$

$$\begin{cases} \nabla^2\Psi = k \cdot \nabla \times \boldsymbol{Q} \,, \\ -\nabla^2\chi = \nabla \cdot \boldsymbol{Q} \,, \end{cases} \tag{2}$$

$$\begin{cases} \boldsymbol{Q}_\Psi = k \times \nabla\Psi \,, \\ \boldsymbol{Q}_\chi = -\nabla\chi \,, \end{cases} \tag{3}$$

where Ψ is the water vapor stream function and χ is the water vapor potential function. Calculations were performed using the following three steps: (1) calculating the water vapor flux $\boldsymbol{Q}$ and its divergence and vorticity fields using the specific humidity q, zonal wind speed u and meridional wind speed v; (2) solving the Poisson equation (using the Successive Over-Relaxation (SOR) method to solve Eq. (2) to obtain the water vapor stream function Ψ and water vapor potential function χ) where SOR is an effective accel-

[a]TCs affecting China mean TCs that produce precipitation over mainland China or any of the two biggest islands of China, Taiwan and Hainan.

erated method in getting a solution of large sparse matrix equations (Buzbee et al., 1970; Kong, 1988; Ding, 1989); and (3) obtaining the divergence (non-rotational) and non-divergence (rotational) components of the horizontal water vapor transport using Eq. (3).

2.2 *The relevant variables of water vapor budget*

The equation for water vapor budget is

$$\frac{\partial q}{\partial t}+\nabla\cdot\boldsymbol{V}q+\frac{\partial}{\partial p}\omega q=-m\,, \tag{4}$$

where m is the condensation quantity of water vapor.

Suppose the atmospheric pressure at bottom and top of the air column be $p_{\rm b}$ and $p_{\rm t}$ respectively and after the integration in the whole air column for a certain region σ, the formula can be changed into

$$\begin{aligned}P-E_{\rm sf}&=-\frac{1}{g}\int_{\sigma}\int_{p_{\rm t}}^{p_{\rm b}}\left(\frac{\partial q}{\partial t}+\nabla\cdot\boldsymbol{V}q+\frac{\partial}{\partial p}\omega q\right)dpd\sigma\\&=-\frac{1}{g}\int_{p_{\rm t}}^{p_{\rm b}}\int_{\sigma}\left(\frac{\partial q}{\partial t}+\nabla\cdot\boldsymbol{V}q+\frac{\partial}{\partial p}\omega q\right)d\sigma dp\,,\end{aligned} \tag{5}$$

where P is the total precipitation and $E_{\rm sf}$ is the evaporation quantity from the underlying surface. The first term on the right-hand side of Eq. (5) is the local variation of the water vapor content and it is generally small; the second term is the convergence of water vapor flux and it is the most important one in water vapor budget; and the third item is the vertical water vapor transport.

Because the water vapor transport in the lower troposphere is the most important component, in addition to integration in the whole air column, the convergence of water vapor flux in the lower troposphere (such as 1000 hPa or 850 hPa and the "thickness" Δp is 1 hPa) was also calculated using the following equations:

$$\begin{aligned}&-\frac{1}{g}\int_{p_{\rm t}}^{p_{\rm b}}\int_{\sigma}(\nabla\cdot\boldsymbol{V}q)\,d\sigma dp\\&=-\frac{1}{g}\int_{\sigma}\nabla\cdot\boldsymbol{V}qd\sigma=-\frac{1}{g}\oint_{\sigma}v_zqdl\\&=-\frac{1}{g}\left(\sum_{j=1}^{k}\tilde{u}_j\tilde{q}_j\Delta l_{\rm e}-\sum_{i=1}^{m}\tilde{v}_i\tilde{q}_i\Delta l_{\rm s}-\right.\\&\left.\sum_{j=1}^{k}\tilde{u}_j\tilde{q}_j\Delta l_{\rm w}+\sum_{i=1}^{m}\tilde{v}_i\tilde{q}_i\Delta l_{\rm n}\right)\,,\end{aligned} \tag{6}$$

where $\Delta l_{\rm e}$, $\Delta l_{\rm s}$, $\Delta l_{\rm w}$ and $\Delta l_{\rm n}$ represent the grid distance for the four borders on the eastern, southern, western, and northern sides, respectively; v_z is the normal component perpendicular to the side border, and m and k are numbers of grids along x and y directions within the calculation zone, respectively. The variables with "$\sim$" are the mean values for the space distance.

The circulation decomposition principle points out that the time average of scalar quadratic term can be decomposed into steady component and transient component, namely $\overline{XY}=\overline{X}\,\overline{Y}+\overline{X'Y'}$. Then it is easy to obtain the time average of the vector $\boldsymbol{V}q$ as

$$\overline{\boldsymbol{V}q}=\overline{\boldsymbol{V}}\,\overline{q}+\overline{\boldsymbol{V}'q'}\,. \tag{7}$$

After substituting Eq. (7) into Eq. (6), then

$$\begin{aligned}&-\frac{1}{g}\int_{p_{\rm t}}^{p_{\rm b}}\int_{\sigma}(\nabla\cdot\overline{\boldsymbol{V}q})d\sigma dp\\&=-\frac{1}{g}\left[\sum_{j=1}^{k}\bar{\tilde{u}}_j\bar{\tilde{q}}_j\Delta l_{\rm e}-\sum_{i=1}^{m}\bar{\tilde{v}}_i\bar{\tilde{q}}_i\Delta l_{\rm s}-\right.\\&\sum_{j=1}^{k}\bar{\tilde{u}}_j\bar{\tilde{q}}_j\Delta l_{\rm w}+\sum_{i=1}^{m}(\bar{\tilde{v}}_i\bar{\tilde{q}}_i\Delta l_{\rm n})-\\&\frac{1}{g}\left(\sum_{j=1}^{k}\overline{\tilde{u}'_j\tilde{q}'_j}\Delta l_{\rm e}-\sum_{i=1}^{m}\overline{\tilde{v}'_i\tilde{q}'_i}\Delta l_{\rm s}-\right.\\&\left.\left.\sum_{j=1}^{k}\overline{\tilde{u}'_j\tilde{q}'_j}\Delta l_{\rm w}+\sum_{i=1}^{m}\overline{\tilde{v}'_i\tilde{q}'_i}\right)\Delta l_{\rm n}\right]\,.\end{aligned} \tag{8}$$

Based on the third item on the right-hand side of Eq. (5), $-\frac{1}{g}\int_{\sigma}\int_{p_{\rm t}}^{p_{\rm b}}\frac{\partial}{\partial p}\omega qdpd\sigma$, the vertical water vapor transport quantity can be conveniently calculated for a certain air column (such as 1000–700 hPa) and its units are also kilograms per second (kg s^{-1}). The term will be zero if ω are both supposed to be zero at the bottom and top layers.

Finally, based on the diagnostic results regarding the possible impact mechanism, a numerical simulation study was conducted. The model applied was the atmospheric circulation model SAMIL (Spectral Atmospheric Model of IAP LASG), developed by the National Laboratory of Atmospheric Science and Geophysical Fluid Dynamics Numerical Simulation of Institute of Atmospheric Physics of Chinese Academy of Sciences (Wang et al., 2007; Bao et al., 2010).

3. Results

3.1 *Variations of affecting China tropical cyclone activities and air–sea interaction*

The frequency of TCs affecting China significantly decreased from 1957 to 2004 (significance level 0.05) with obvious interannual variations. Although the

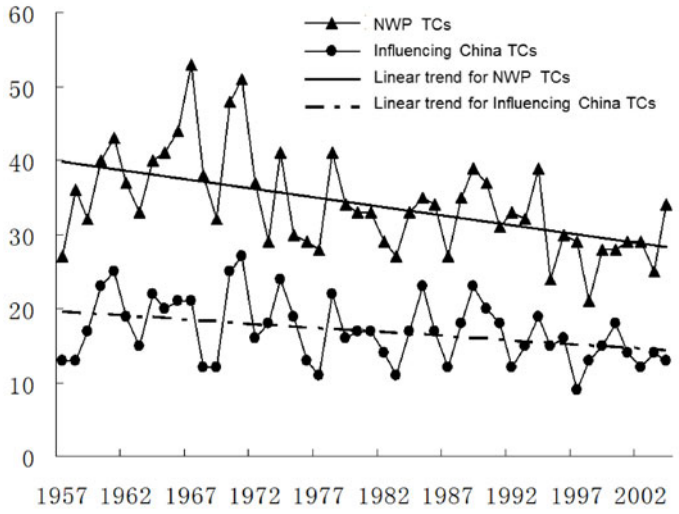

Fig. 1. Variations of the frequency of Northwest Pacific (NWP) TCs and TCs affecting China.

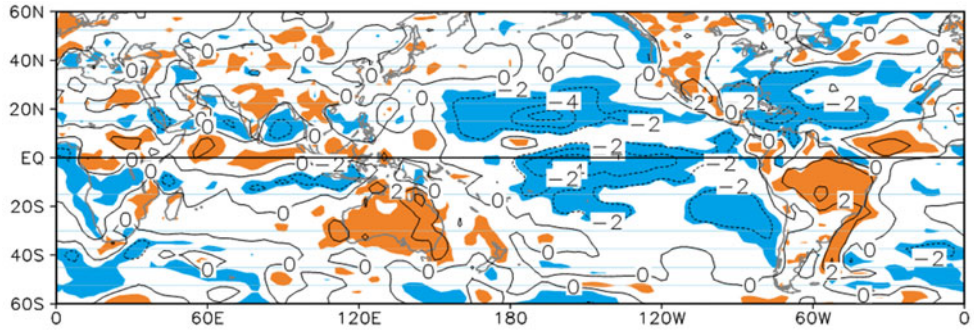

Fig. 2. Linear trend (unit: W m^{-2} yr^{-1}) distribution of latent heat flux (June–October) from 1958 to 2001. The orange shaded areas indicate significant positive trends at the 99% confidence level; the blue areas indicate significant negative trends at the 99% confidence level.

maximum of 27 occurred in 1971, there was no obvious interdecadal variation. In addition, STI-CMA TC dataset also shows that the TC frequency in the Northwest Pacific decreased remarkably during this period (Fig. 1), with obvious interdecadal variation.

The linear trend of latent heat flux for the main TC active period (June–October) was analyzed to find the key region of air–sea interaction (Fig. 2). The distribution of the linear trend is globally inhomogeneous in the tropics and the subtropics, with significant decreasing trends over most of the central and eastern Pacific, tropical zone of the South Indian Ocean, and the western North Atlantic Ocean, and slightly increasing trends in parts of the remainder of the tropics and the subtropics.

3.2 *Correlation analysis*

Correlation analysis between the frequency of TCs affecting China and the latent heat flux field for June to October shows that the main areas with significant correlation appear in the central tropics and subtropics of the North Pacific, the eastern tropics of the South Pacific, the Indian Ocean south to Indonesia, and parts of the eastern tropics of the South Pacific (Fig. 3). Considering the distribution of average latent heat flux, two key areas of latent heat flux affecting the Northwest Pacific TC activity can be initially determined (Fig. 3): the central tropics and subtropics of the North Pacific (Area 1: 10°–30°N, 150°E–150°W) and the eastern tropics of the South Pacific (Area 2: 0°–20°S, 180°–90°W).

The variations of the mean latent heat fluxes in the two key areas (Figs. 4a, b) both show significant decreasing trends in the past 40 years and more. In the central tropics and subtropics of the North Pacific (Area 1) it decreased by an average of 2.5 W m^{-2} each year, whereas it decreased 2.7 W m^{-2} in the eastern tropics of the South Pacific (Area 2). Correlation anal-

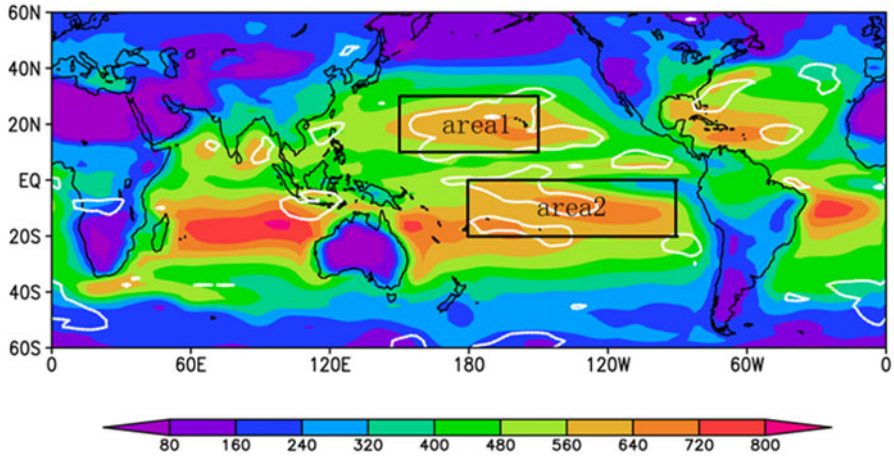

Fig. 3. Distribution of the averaged latent heat flux (June–October) from 1958 to 2001 and the correlation coefficient between the frequency of TCs affecting China and the latent heat flux field. The shaded area indicates the averaged latent heat flux (units: W m^{-2}); the white contours indicate the correlation coefficient at a significance level of 0.05; and the black boxes indicate the key areas in this study.

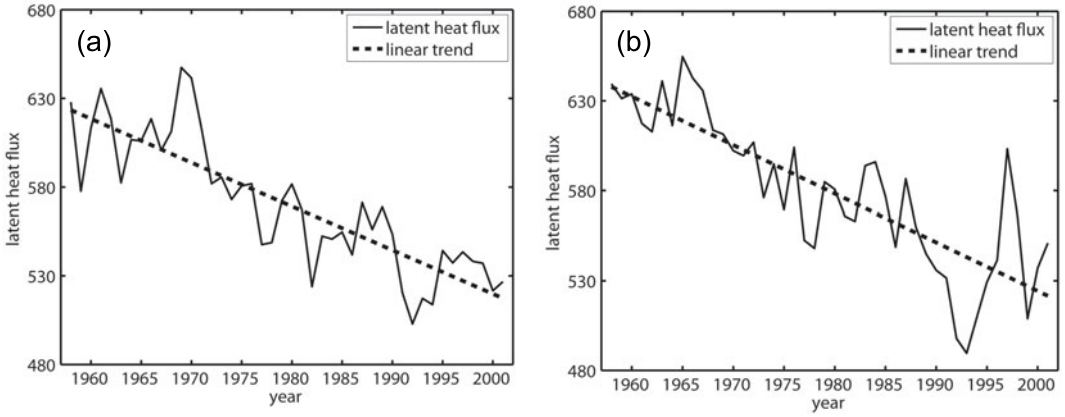

Fig. 4. The two key areas for latent heat flux and their series of area mean latent heat fluxes (units: W m^{-2}): (a) the series for Area 1, (b) the series for Area 2.

ysis shows that correlation coefficients between annual frequency of TCs affecting China and the two series of Area 1 and Area 2 are 0.37 and 0.17, respectively; the former is significant (significance level 0.05), while the latter is insignificant. In addition, the correlation coefficient between the two series of Area 1 and Area 2 is 0.81, meaning that the variation of the latent fluxes in the two areas are highly consistent, while the air–sea interaction in the two key areas may have obvious differences that affect or modulate the activity of TCs affecting China.

Further analysis was conducted on two variables that may affect latent heat flux in Area 1: air–sea humidity difference ($q_{\text{ocean}} - q_{\text{atm}}$) and average wind $|U|$. The correlation coefficients between the latent heat flux and the two factors are 0.64 and 0.13, respectively. Only the former is significant, which indicates that the decreasing trend of latent heat flux in Area 1 may be mainly caused by the decrease of air–sea humidity difference.

3.3 *Analysis of moisture budget*

The western North Pacific was divided into two areas: South China Sea (SCS, 5°–20°N, 110°–120°E) and the Northwest Pacific (NWP, 5°–25°N, 120°–180°E). The moisture budget analysis (Fig. 5) performed for the two areas based on layer integration shows that the two areas are moisture sinks (10.55×10^{12} kg d^{-1} for the SCS and 47.49×10^{12} kg d^{-1} for the NWP). However, these two areas largely differ in moisture budget. The western and southern SCS boundaries are the two moisture inflows

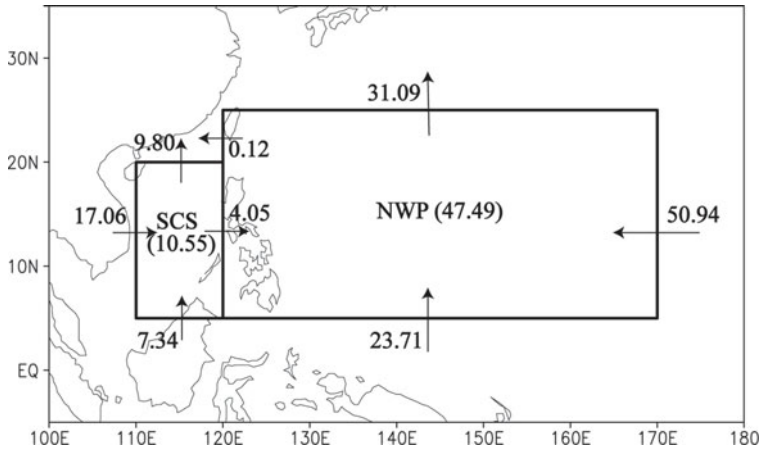

Fig. 5. A sketch showing moisture budget in the SCS and the NWP (units: 10^{12} kg d^{-1}). SCS (5°–20°N, 110°–120°E); NWP (5°–25°N, 120°–170°E).

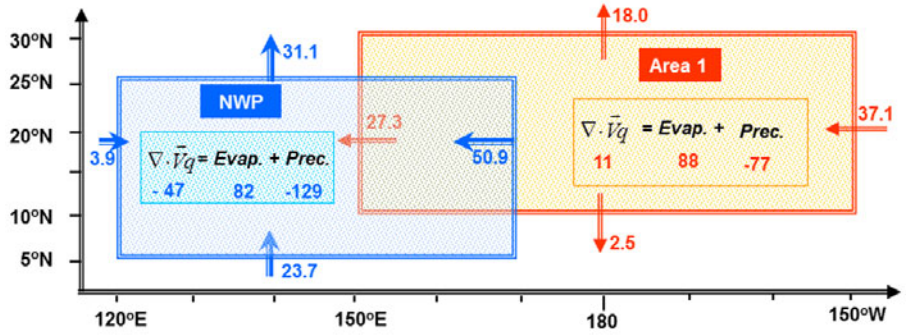

Fig. 6. Water cycle in typhoon season (June–October) in the Northwest Pacific and Area 1 (units: 10^{12} kg d^{-1}).

(17.06×10^{12} kg d^{-1} and 7.34×10^{12} kg d^{-1}, respectively). Notably, the western boundary was the major source of moisture inflow, and the eastern and northern boundaries were moisture outflows (northward outflow was 9.8×10^{12} kg d^{-1} and the outflow from the eastern boundary into the NWP was 4.05×10^{12} kg d^{-1}). For the NWP, moisture inflows were detected from three directions, i.e. from eastern, southern and western boundaries [per unit inflow values: 50.94×10^{12} kg d^{-1}, 23.71×10^{12} kg d^{-1}, and 3.93×10^{12} kg d^{-1} ($=4.05–0.12\times10^{12}$ kg d^{-1}), respectively], while the northern boundary exhibited the only moisture outflow (31.09×10^{12} kg d^{-1}).

Therefore, the NWP, a TC genesis region, was identified as a sink of moisture in the typhoon season (June–October). Using ERA40 reanalysis data, further analysis shows that the sea surface evaporation in the NWP only accounted for 63.6% (82×10^{12} kg d^{-1}, see Fig. 6) in total precipitation (129×10^{12} kg d^{-1}). Therefore, the moisture inflow ($\approx47\times10^{12}$ kg d^{-1}) from elsewhere became another important source of moisture in the typhoon season, i.e., moisture transport ($=50.9\times10^{12}$ kg d^{-1}) from upper-stream tropical and subtropical Pacific (Area 1), was a major source of moisture.

A moisture analysis of Area 1 (Fig. 6) shows that the large amount of sea surface evaporation (88×10^{12} kg d^{-1}) in the region provides supplementary moisture (-77×10^{12} kg d^{-1}) for precipitation, and the rest of the moisture transfers to the westward, southward, and northward areas as another important source of moisture, out of which the moisture transport (27×10^{12} kg d^{-1}) to its western boundary is the largest. On a given average temporal scale, the characteristics of water cycle over the Northwest Pacific suggest that a large amount of moisture evaporated from Area 1 is transported along the prevailing easterly stream to the NWP, as a continuous supply of moisture for TC genesis in the region.

Figure 7 is prepared to further analyze the trend

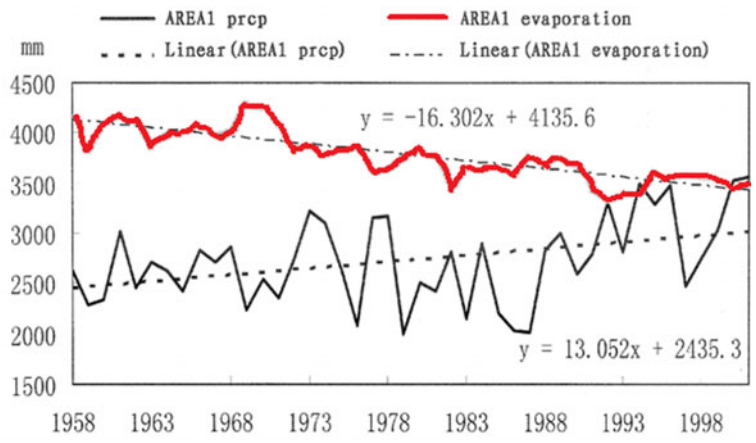

Fig. 7. Evolutions of mean precipitation and evaporation in Area 1 (units: mm).

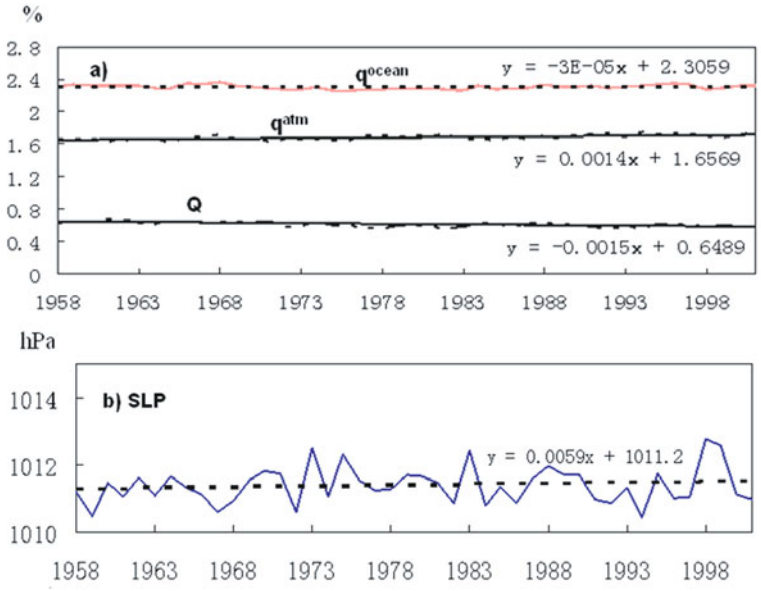

Fig. 8. Variations of sea-surface specific humidity ($q_{\rm ocean}$), specific humidity content ($q_{\rm atm}$), air–sea specific humidity difference (H) and sea level pressure (SLP) in Area 1.

of outgoing moisture transport in Area 1. The analysis results show that precipitation (P) gradually increased, while the sea surface evaporation ($E_{\rm sf}$) linearly decreased in Area 1 during the past 40 years. Thus, outgoing moisture transport $\nabla \cdot \boldsymbol{V}q = E_{\rm sf} - P$ was significantly reduced during the past few decades. Therefore, the reduction of outgoing moisture transport in Area 1 may be a major reason for the decrease in frequency of typhoons over the Northwest Pacific.

What has caused the significant decrease of sea-surface evaporation in Area 1 during the past 44 years? As the moisture conductivity coefficient C_q changes relatively small in the tropical oceans, from perspective of the overall dynamic transport, sea surface evaporation flux $\boldsymbol{F}$ is proportional to the surface (at 10 m) wind speed $\boldsymbol{V}$ and air–sea specific humidity difference $H(= q_{\rm ocean} - q_{\rm atm})$, i.e., $\boldsymbol{F} \propto \boldsymbol{V}H$. The analysis suggests that the major cause for the variation in sea-surface evaporation was the significant decrease of the air–sea specific humidity difference (Fig. 8a). In other words, on one hand, this variation was due to the general increase of sea level pressure (Fig. 8b) in this area, which leads to slight decline of the sea-surface specific humidity (Fig. 8a). On the other hand, the more important aspect was the significant increase of specific humidity content (dew point) in the atmosphere in the region (Fig. 8a).

In general, in the past 44 years, with global warm-

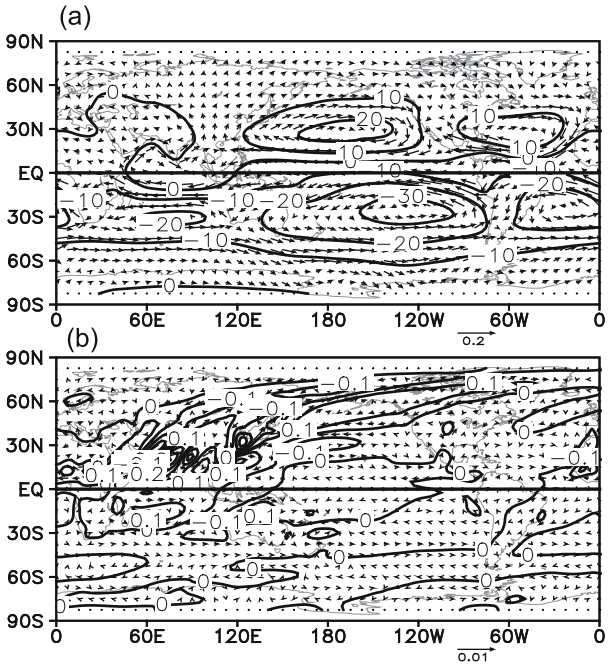

Fig. 9. Average stream function (unit: 10^5 kg s^{-1}) and non-divergence component (arrow, units: kg m^{-1} s^{-1}) of moisture transport at 1000 hPa for an unit atmospheric layer from June to October: (a) constant component; (b) transient component.

ing, the moisture content of the atmosphere near the sea surface in Area 1 has increased (Fig. 8a), which has led to a decrease of sea-surface evaporation in the same area. Consequently, the moisture transport from Area 1 to the Northwest Pacific has declined, which might have reduced the frequency of typhoon genesis in the NWP.

3.4 *Analysis using stream function and potential function*

Further analysis of stream and potential functions showed that trade winds from the tropical Atlantic Ocean to the Pacific have a significant role in moisture transport, especially in the tropical Pacific, which is consistent with the analysis of moisture transport from Area 1 to the Northwest Pacific as noted above.

Figure 9 shows the distribution of non-divergence moisture flux at 1000 hPa during June–October. The non-divergence moisture flux represents the moisture components that are transported along isobars. The constant component (Fig. 9a) shows that the strongest moisture flux occurs over the oceans. Overall, corresponding to the vortex, the moisture fields in the subtropical Pacific and Atlantic in the Northern Hemisphere and the entire tropical Indian Ocean are characterized by a clockwise vortex structure. On the contrary, the moisture flux fields over the Central and Eastern tropical Pacific and Atlantic in the Southern Hemisphere show a counter-clockwise vortex structure. Notably, trade winds from the tropical Atlantic to the Pacific have a significant role in moisture transport, especially in the tropical Pacific, which is consistent with the analysis of moisture transport from Area 1 to the Northwest Pacific, as noted above. Compared to the constant component, the transient component is a small value, which is generally smaller than the constant component by an order of 2 or 3, with no obvious center over the Pacific. Another analysis was made on mean non-rotational moisture flux at 1000 hPa in June–October (figure omitted). The analytical results show that the Central and Western Pacific tropics have been identified as a sink of moisture. Based on the above analyses, it is clear that the typhoon activity area in the entire Northwest Pacific (including SCS) is a moisture sink. Moisture mainly comes from three sources: moisture transport by trade wind over the Central and Eastern tropical Pacific, by southwest Asian monsoonal flow from the west, and by cross-equatorial flow from the Southern Hemisphere. The moisture outflow is mainly in two directions: northward transport by southwest Asian monsoon, and northward transport by southeastern flow from the southwestern side of the West Pacific subtropical high.

3.5 *A potential impact mechanism*

A previous analysis (Li, 2000) pointed out that the maximum heating effect of the ocean to the atmosphere often does not occur directly over the region with the maximum evaporation. From this analysis, it is quite clear that the central North Pacific tropics and subtropics (Area 1) is a key area for air–sea interaction, which is closely related to TC activity in the Northwest Pacific, including the South China Sea. When latent heat flux weakened in Area 1, the moisture transported westward by low-level trade wind weakened. Correspondingly, in the Northwest Pacific, which is a sink of moisture, after external moisture condensed through low-level convergence and was pushed upward, then released latent heat decreased. Then low-level vorticity, low- and mid-level moisture, and low-level convergence and high-level divergence weakened. These changes favored decreased TC activity in the Northwest Pacific, thereby decreasing the frequency of TCs affecting China. Conversely, when latent heat flux strengthened in Area 1, the moisture transported westward by low-level trade wind strengthened. Correspondingly in the Northwest Pacific, after external moisture condensed through low-level convergence and was pushed upward, then released latent heat increased. Then low-level vorticity, low- and mid-level moisture, low-level convergence,

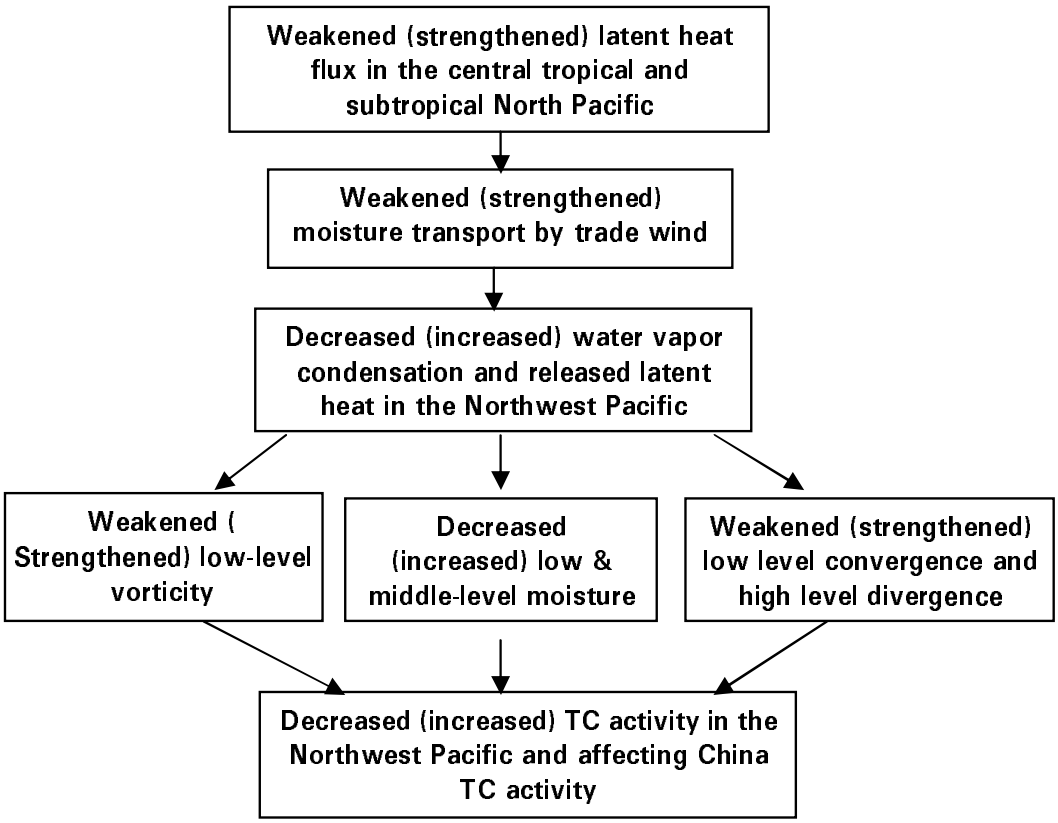

Fig. 10. Conceptual chart of the potential impact mechanism.

and high-level divergence strengthened. These changes favored increased TC activity in the Northwest Pacific, thereby increasing the frequency of TCs affecting China. Figure 10 shows a conceptual chart of these potential impact mechanisms.

4. Modeling of the potential impact mechanism

Based on this analysis outlined in section 3, we verified that latent heat flux in a key area potentially affects the TC activity in the Northwest Pacific using a numerical model.

4.1 *Experimental design*

The model used in this study was SAMIL; it uses a horizontally rhomboidal truncation with a resolution of 42 waves, being equal to a grid of 2.8125° (longitude) ×1.67° (latitude). There are 26 vertical layers, with the lowest level being a pure σ coordinate, the highest seven levels being pure isobaric surface coordinates, and hybrid coordinates between them. Physical processes include UKMO's radiation scheme (Edwards and Slingo, 1996), non-local atmospheric boundary layer parameterization scheme (Holtslag and Boville, 1993), Slingo's diagnostic cloud scheme (Slingo, 1987), and multi-gravity wave drag parameterization (Palmer et al., 1986).

In the control test, the average ECMWF reanalysis data fields in January from 1958 to 2001 are selected as initial fields, including height, temperature, radial wind, zonal wind, relative humidity, and surface temperature.

With a 6-year integration in a control run, a stable state was reached. Therefore, for the sensitivity test, the output data obtained on 1 June of year 6 of the control experiment were selected as initial fields. At the same time, the latent heat flux of each step in the two key areas from 1 June to 31 October was doubled (doubled experiment for short) and halved (halved experiment for short), respectively, for monthly mean ambient fields in June–October.

4.2 *Sensitivity experiment targeted to Area 1*

Because the control and sensitivity experiments reached stability in a 6-year integration, a comparison between environmental variables averaged from 1 June to 31 October of these experiments made it possible to determine whether heat flux-halving and doubling experiments were favorable for TC activity.

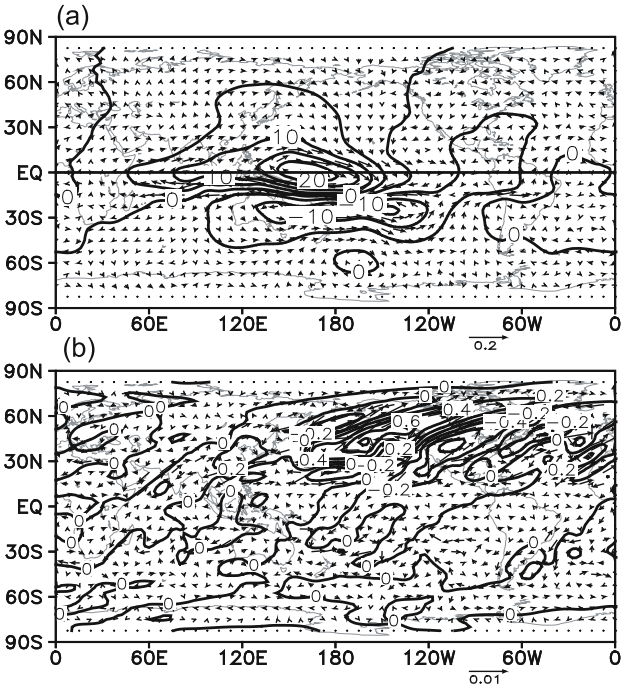

Fig. 11. Difference distribution of stream function (unit: 10^5 kg s^{-1}) and non-divergence component (arrows, units: kg m^{-1} s^{-1}) of moisture transport at 1000 hPa in June–October between experiments by halving and doubling latent heat flux in Area 1: (a) constant component; (b) transient component.

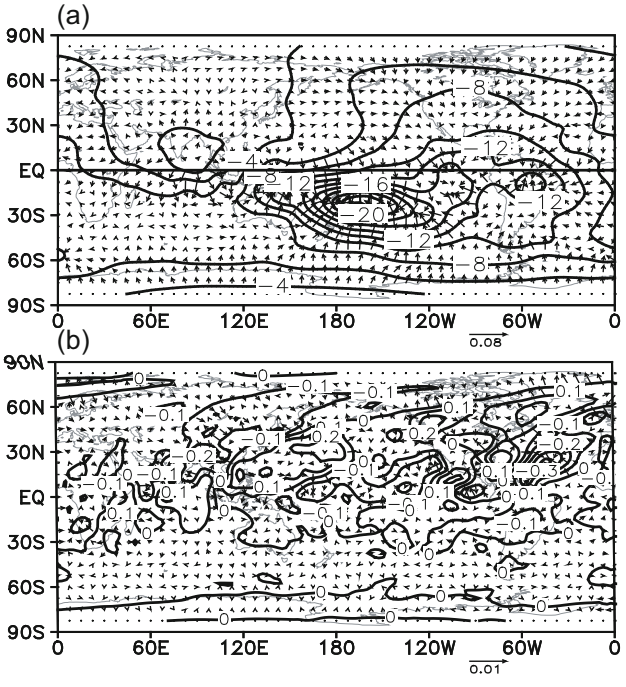

Fig. 12. Difference distribution of potential function (unit: 10^5 kg s^{-1}) and non-rotational component (arrows, unit: kg m^{-1} s^{-1}) of moisture transport at 1000 hPa in June–October between experiments by halving and doubling latent heat flux in Area 1: (a) constant component; (b) transient component.

Figure 11 shows a difference of the stream function and non-divergence of moisture transport at 1000 hPa between the halved and doubled experiments. The constant component (Fig. 11a) shows that the former experiment was conducive to emergence of a strong clockwise vortex in moisture transport on the surface of central Western Pacific tropics, which weakened westward moisture transport from the Area 1 to the NWP. The results indicate that reduced latent heat flux in Area 1 significantly weakened moisture transport to the Northwest Pacific. Conversely, when latent heat flux increased in Area 1, the westward moisture transport from the region was significantly enhanced, i.e., enhanced moisture was transported from Area 1 to the Northwest Pacific. The stream function of the transient component and the non-divergence component (Fig. 11b) was clearly much smaller than the constant component over the tropical and subtropical Pacific.

Figure 12 gives differences of both potential function and non-rotational component of vapor transport at 1000 hPa between these two experiments. The non-rotational component was small, but it could adjust both source and sink of moisture. As shown in Fig. 12a, the former experiment was conducive to generating a strong moisture convergence zone in central and western parts of the South Pacific, i.e., the reduction of latent heat flux in Area 1 helped to demonstrate the role of abnormal moisture sink in the region. At the same time, obvious moisture transport divergence appeared in the TC activity area of the Northwest Pacific, suggesting that the role of original moisture sink had weakened, i.e., when the moisture evaporation in Area 1 was reduced, it directly led to the weakening of moisture sink in the Northwest Pacific. On the contrary, when the latent heat flux was enhanced in Area 1, the moisture transport formed a convergence in the anomalous field in the Northwest Pacific, i.e., the increasing moisture evaporation in Area 1 directly led to enhanced original moisture sink in the TC activity area. Compared with the constant component, the transient component (Fig. 12b) was smaller by an order of 2, without significantly impacting the Northwest Pacific.

Further analysis suggests that over the Northwest Pacific, the average daily precipitation in the former experiment was 7.0 mm less than that in the latter experiment in Area 1, while it increased by 1.1 mm d^{-1} in the SCS. This shows that when the latent heat flux weakened in Area 1, the moisture condensation and

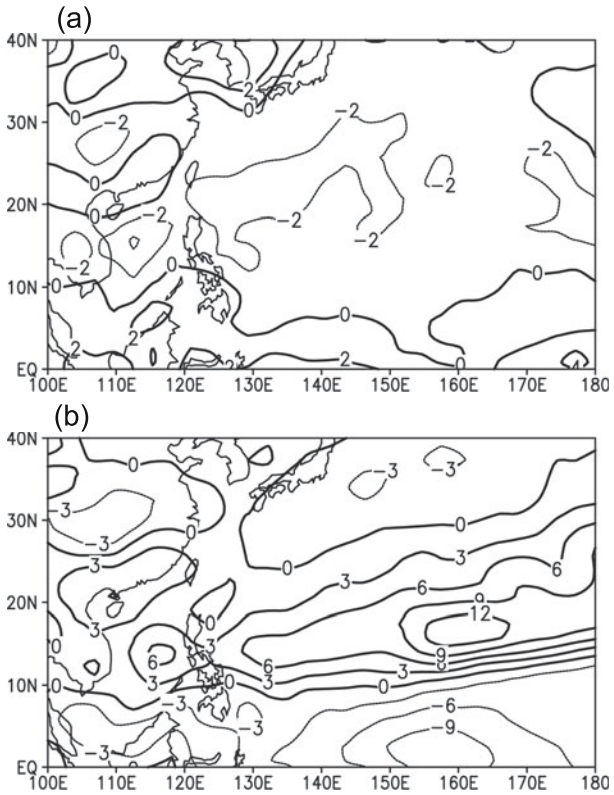

Fig. 13. Mean vorticity differences (unit: 10^{-6} s^{-1}) at 850 hPa in June–October between sensitivity experiments and control test targeted to Area 1: (a) heat flux-halving experiment; (b) heat flux-doubling experiment.

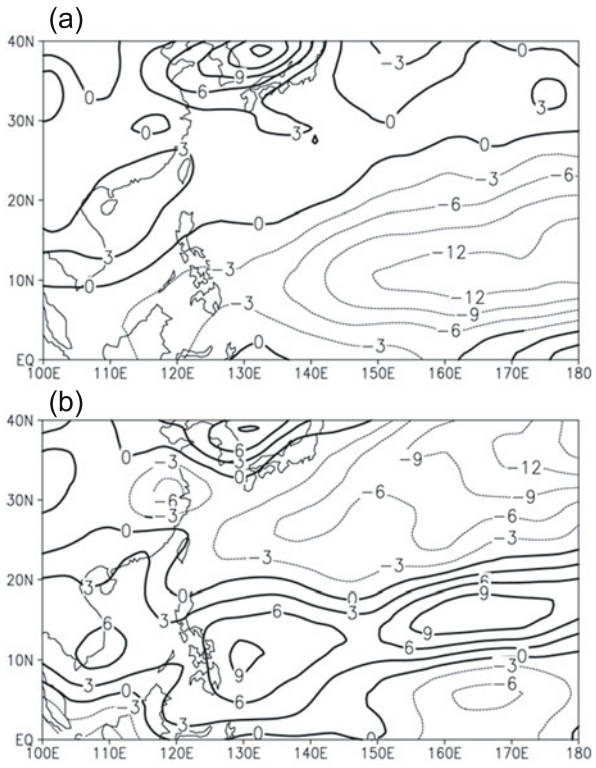

Fig. 14. Relative humidity differences (units: %) at 700–500 hPa in June–October between sensitivity experiments and the control test targeted to Area 1: (a) heat flux-halving experiment; (b) heat flux-doubling experiment.

latent heat release decreased in the Northwest Pacific, while the moisture condensation and latent heat release over the SCS slightly increased. When the latent heat flux strengthened in Area 1, the moisture condensation and latent heat release increased in the Northwest Pacific, while the moisture condensation and latent heat release over the SCS slightly decreased.

Figure 13 presents the distribution of vorticity difference at 850 hPa in June–October between sensitivity and control tests. It is clear that the vorticity in the lower atmosphere in most of the South China Sea and the northern part of the Northwest Pacific north of 5°N weakened in the experiment when the latent heat was halved, which was unfavorable for TC genesis in general. In the experiment that doubled the value, over the Northwest Pacific north of 10°N (including the SCS), the lower tropospheric vorticity was strengthened unusually, which was favorable for TC genesis and development.

The distribution of relative humidity differences between sensitivity experiments and control tests are given in Fig. 14. The humidity in mid- and low-level atmosphere over most of the Northwest Pacific was reduced in the heat-halving experiment, which was unfavorable for TC development. On the contrary, the humidity was relatively higher in the northern South China Sea. From the heat-doubling experiment, the humidity over the vast Northwest Pacific to the south of 20°N (including South China Sea) increased, which provided the right conditions for active TCs.

The mean divergence differences between heat flux-halving and -doubling experiments (Fig. 15) show that compared with the heat-doubling experiment, divergence at 1000 hPa in the Northwest Pacific (including SCS) was clearly enhanced in heat-halving experiment, while convergence at 200 hPa generally experiences an increased. This shows that abnormal convergence or divergence in both the high- and low-level atmosphere due to reduced latent heat flux in Area 1 is unfavorable for TC genesis and development over the Northwest Pacific (including the SCS), and also means that abnormal divergence or convergence in both the high- and low-level atmosphere in heat-doubling experiment is favorable for TC genesis and development over the Northwest Pacific (including the SCS).

Numerical simulations further confirmed that TC activity over the Northwest Pacific was very sensitive to the air–sea interaction in Area 1 (Fig. 10). The ana-

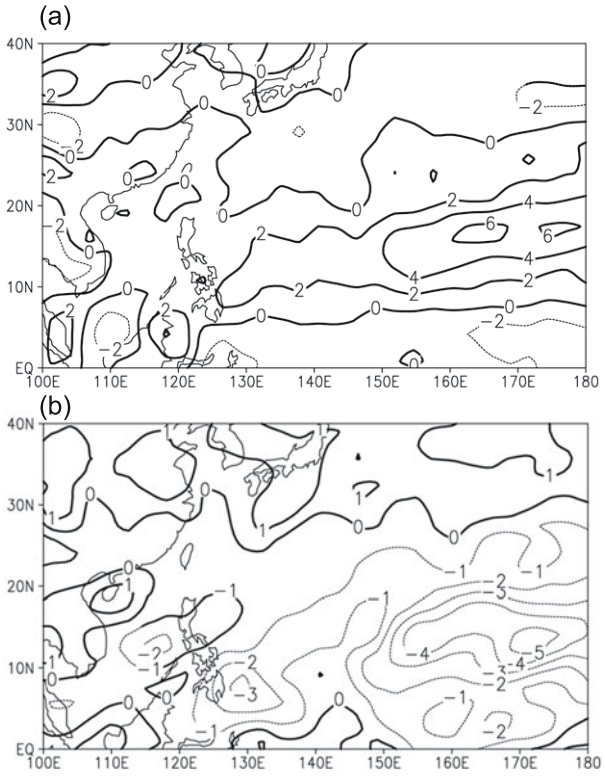

Fig. 15. Mean divergence differences (units: 10^{-6} s^{-1}) in June–October between heat flux-halving and -doubling experiments targeted to Area 1: (a) 1000 hPa; (b) 200 hPa.

lysis also shows some regional differences of TC activity over the whole the NWP region in responding to air–sea interactions in Area 1, while the response of the South China Sea region was insignificant.

4.3 *Sensitivity experiment targeted to Area 2*

Similar to the previous analysis for Area 1, analysis for Area 2 was performed. For brevity, only conclusions are given here.

The simulation tests showed that TC activity in June–October over the Northwest Pacific (including the SCS) was not sensitive to air–sea interaction in the eastern part of the South Pacific tropics (Area 2). When the latent heat flux in Area 2 weakened or enhanced, it directly weakened or strengthened the moisture transport to the Southwest Pacific. For the Northwest Pacific, latent heat flux impacts were driven by the moisture transport by cross-equator flows and were mainly confined to the southeastern part of the NWP, thus they were indirect and partial for the entire NWP. Further analysis showed that, when the latent heat flux in Area 2 increased or decreased, the atmospheric environmental conditions such as the mid- and low-level vorticity/humidity, low-level convergence and high-level divergence fields underwent little change, suggesting that the impacts of Area 2 on TC activity in the Northwest Pacific (including SCS) and even on TC activity affecting China are very limited.

5. Discussion and summary

This study focused on revealing the mechanisms of air–sea interaction related to TC activity affecting China. The main conclusions can be summarized as follows:

(1) The TC activity area in the entire Northwest Pacific (including South China Sea) is a moisture sink, with moisture mainly coming from three sources: moisture transport by trade wind from the central and eastern tropical Pacific, by the Southwest Asian Monsoon, and by the cross-equator flows from the Southern Hemisphere. The moisture outflows are mainly from two sources: the Southwest Asian Monsoon transporting moisture from the north bound of the region to the north, and southeasterly flows from southwest of the West Pacific Subtropical High to the north. From the perspective of the differences in moisture budget, the region can be divided into two areas: South China Sea (SCS, 5°–20°N, 110°–120°E) and the Northwest Pacific.

(2) The diagnostic analysis shows that the central North Pacific tropics and subtropics (Area 1: 10°–30°N, 150°E–150°W) was one of the key areas of air–sea interaction in terms of the impacts on TC activity. In the past 44 years (1958–2001), under global warming, the near sea surface moisture content increased in Area 1, resulting in a decreasing humidity difference between sea and air, eventually leading to reduced evaporation and latent heat flux in this area.

(3) Diagnostic analysis and modeling studies suggested that Area 1 has an important role in modulating TC activity over the Northwest Pacific and on TC activity that affects China. The associated mechanism may be described as follows: When latent heat flux weakens in Area 1, the moisture transported westward by low-level trade wind weakens. Correspondingly in the Northwest Pacific, which is a sink of moisture, after external moisture condenses through low-level convergence and is pushed upward, then released latent heat decreases. Then low-level vorticity, low- and mid-level moisture, and low-level convergence and high-level divergence weaken. These changes favor a decrease in TC activity in the Northwest Pacific, thereby decreasing the frequency of TCs that affect China. Conversely, when latent heat flux strengthens in Area 1, the moisture transported westward by low-level trade wind strengthens. Correspondingly in the Northwest Pacific, after external moisture condenses through low-

level convergence and is pushed upward, then released latent heat increases. Then low-level vorticity, low- and mid-level moisture, and low-level convergence and high-level divergence strengthen. These changes favor increased TC activity in the Northwest Pacific, thereby increasing the frequency of TCs that affect China. The analysis also showed certain regional differences in responding to TC activity over the western North Pacific to the air–sea interaction in Area 1, insufficient responses were mainly found in the South China Sea.

In the past four decades, the frequency of TC activity affecting China has trended significantly downward. Meanwhile, the two key areas for air–sea interaction over the Pacific also underwent weakening trend. Our diagnostic analysis and modeling studies suggest that air–sea interaction over the central North Pacific tropics and subtropics (Area 1) has an important role in modulating TC activity over the whole region, and even TC activity affecting China. But according to our results, over the eastern part of the South Pacific tropics (Area 2), the air–sea interaction has rather limited impacts on TC activity in the western North Pacific. This analysis and modeling study also showed that in the past four decades, the weakening trend of latent heat release over the region was consistent with the decreasing TC frequency the western North Pacific based on CMA datasets. This trend may explain the decreasing TC frequency over the Northwest Pacific and in China's offshore. This analysis reveals the mechanism of air–sea interaction in modulating TC genesis conditions, which have direct or indirect impacts on China. Further in-depth investigation is required for many issues, such as how it modulates and impacts TC tracks approaching mainland China.

Acknowledgements. The authors gratefully acknowledge the two anonymous reviewers whose valuable comments contributed a great deal to improving the quality of this paper. Meanwhile, the authors would like to express their sincere thanks to Dr. WU Liguang , Dr. JIANG Haiyan, and Mr. Joseph ZAGRODNIK for their help in modifying the grammar in the manuscript. This work was supported by the R&D Special Fund for Public Welfare Industry (meteorology) (Grant No. GYHY200806009) and the National Natural Science Foundation of China (Grant Nos. 40775046, 40730106).

REFERENCES

Bao, Q., G. X. Wu, Y. M. Liu, J. Yang, Z. Z. Wang, and T. J. Zhou, 2010: An introduction to the coupled model FGOALS1.1-s and its performance in East Asia. *Adv. Atmos. Sci.*, **27**(5), 1131–1142, doi: 10.1007/s00376-010-9177-1

Buzbee, B. L., G. H. Golub, and C. W. Nielson, 1970: The method of odd/even reduction and factorization with application to Poisson's equation, Part II. STAN-CS-70-155, LA-4288, Los Alamos Scientific Laboratory.

Chan, J. C. L., and K. S. Liu, 2004: Global warming and Western North Pacific typhoon activity from an observational perspective. *J. Climate*, **17**, 4590–4602.

Chan, J. C. L., 2006: Comments on "Changes in Tropical Cyclone Number, Duration, and Intensity in a Warming Environment". *Science*, **311**, 1713b.

Chan, J. C. L., 2008: Decadal variations of intense typhoon occurrence in the western North Pacific. *Proc. Royal Soc. London*, **464**, 249–272.

Chen, L. S., and Y. H. Ding, 1979: *A Panorama of Typhoon Activities in the Western North Pacific*. Science Press, Beijing, 109pp. (in Chinese)

Ding, Y. H., 1989: *Diagnosis Methods of Weather Dynamics*. Science Press, Beijing, 293pp. (in Chinese)

Ding, Y. H., and G. Q. Hu, 2003: A study on water vapor budget over China during the 1998 severe flood periods. *Acta Meteorologica Sinica*, **61**(2), 129–145. (in Chinese)

Edwards, J. M., and A. Slingo, 1996: Studies with a flexible new radiation code. I: Choosing a configuration for a large-scale model. *J. Roy. Meteor. Soc.*, **122**, 689–719.

Haarsma, R. J., J. F. B. Mitchell, and C. A. Senior, 1993: Tropical disturbances in a GCM. *Climate Dyn.*, **8**, 247–257.

Holtslag, A. A. M., and B. A. Boville, 1993: Local versus nolocal boundary-layer diffusion in a global climate model. *J. Climate*, **6**, 1825–1842.

Hoyos, C. D., P. A. Agudelo, P. J. Webster, and J. A. Curry, 2006: Deconvolution of the factors contributing to the increase in global hurricane intensity. *Science*, **312**, 94–97.

Kong, F., 1988: Comparisons between FFT and SOR on Solving the 2-D Poisson Equations. *Scientia Meteorologica Sinica*, **18**(1), 19–28. (in Chinese)

Krishnamurti, T. N., T. R. Correa, M. Latif, and G. Daughenbaugh, 1998: The impact of current and possibly future sea surface temperature anomalies on the frequency of Atlantic hurricanes. *Tellus*, **50**, 186–210.

Li, C. Y., 2000: *Introduction to Climate Dynamics*. Meteorological Press, Beijing, 515pp. (in Chinese)

Li, Y., and L. S. Chen, 2005: Numerical study on impacts of boundary layer fluxes over wetland on sustention and rainfall of land falling tropical cyclone. *Acta Meteorologica Sinica*, **63**(5), 683–694. (in Chinese)

Ooyama, K., 1969: Numerical simulation of the life cycle of tropical cyclone. *J. Atmos. Sci.*, **25**(1), 3–40.

Palmén, E. H., 1948: On the formation and structure of tropical cyclones. *Geophysica*, **3**, 26–38.

Palmer, T. N., G. J. Shutts, and R. Swinbank., 1986: Alleviation of a systematic westerly bias in general circulation and numerical weather prediction models through an orographic gravity wave drag parameterization. *Quart. J. Roy. Meteor. Soc.*, **112**, 1001–1039.

Ren, F., J. Liang, G. Wu, W. Dong, and X. Yang., 2012:

Reliability analysis of climate change of tropical cyclone Aactivity over the western North Pacific. *J. Climate,* **24**, 5887–5898.

Slingo, J. M., 1987: The development and verification of a cloud prediction scheme for the ECMWF model. *Quart. J. Roy. Meteor. Soc.*, **113**, 899–927.

Wang, Z. Z., R. C. Yu, Q. Bao, T. J. Zhou, Y, M, Liu, P. F. Wang, and G. X. Wu, 2007: A comparison of the atmospheric circulations simulated by the FGOALS-s and SAMIL. *Chinese J. Atmos. Sci.*, **31**(2), 202–213. (in Chinese)

Zhang, F. Q., H. W. Du, and Q. R. Jiang, 1994: A numerical study of the boundary layer effect on mature typhoon. *Journal of Tropical Meteorology*, **10**(2), 108–114. (in Chinese)

Zhou, T. J., and X. H. Zhang, 2002: The atmosphere–ocean heat flux exchange in the Indian Ocean. *Chinese J. Atmos. Sci.*, **26**(2), 161–170. (in Chinese)